

Article

Effects of Changes in Biopolymer Composition on Moisture in Acetylated Wood

Tiantian Yang ^{1,2,*}, Emil Englund Thybring ³ , Maria Fredriksson ⁴ , Erni Ma ²,
Jinzhao Cao ² , Ramūnas Digaitis ⁴ and Lisbeth Garbrecht Thygesen ³ 

¹ College of Materials Science and Engineering, Nanjing Forestry University, Nanjing 210037, China

² Department of Wood Science and Technology, Beijing Forestry University, Beijing 100083, China; maerni@bjfu.edu.cn (E.M.); caoj@bjfu.edu.cn (J.C.)

³ Department of Geosciences and Natural Resource Management, University of Copenhagen, DK-1958 Frederiksberg C, Denmark; eet@ign.ku.dk (E.E.T.); lgt@ign.ku.dk (L.G.T.)

⁴ Division of Building Materials, Lund University, SE-221 00 Lund, Sweden; maria.fredriksson@byggtek.lth.se (M.F.); ramunas.digaitis@byggtek.lth.se (R.D.)

* Correspondence: bjfu100514327@163.com

Received: 10 May 2020; Accepted: 24 June 2020; Published: 29 June 2020



Abstract: To investigate the effects of changes in biopolymer composition on moisture in acetylated poplar wood (*Populus euramericana* Cv.), the acetylation of control wood was compared to the acetylation of wood with reduced hemicellulose or lignin content (about 9% reduction of total specimen dry weight in both cases). Time-domain nuclear magnetic resonance relaxometry of water-saturated wood gave spin–spin relaxation times (T_2) of water populations, while deuteration in a sorption balance was used to characterize the hydroxyl accessibility of the wood cell walls. As expected, the acetylation of pyridine-swelled wood reduced hydroxyl accessibility and made the cell wall less accessible to water, resulting in a reduction of cell wall moisture content by about 24% compared with control wood. Hemicellulose loss per se increased the spin–spin relaxation time of cell wall water, while delignification had the opposite effect. The combined effect of hemicellulose removal and acetylation caused more than a 30% decrease of cell wall moisture content when compared with control wood. The acetylated and partially delignified wood cell walls contained higher cell wall moisture content than acetylated wood. An approximate theoretical calculation of hydroxyl accessibility for acetylated wood was in the low range, but it agreed rather well with the measured accessibility, while acetylated and partially hemicellulose-depleted and partially delignified wood for unknown reasons resulted in substantially lower hydroxyl accessibilities than the theoretical estimate.

Keywords: acetylation; biopolymer composition change; hemicellulose; lignin; moisture; wood

1. Introduction

Wood is receiving more and more attention as a building material due to its low carbon footprint [1–3]. However, wood is a hygroscopic material, and the moisture content therefore changes depending on the relative humidity of the air [4]. Many properties of wood, such as dimensional stability [5], mechanical properties [6], and resistance toward biological degradation [7] are affected by the moisture content in wood [8,9]. The applicability of wood and wood products is consequently challenged by moisture changes.

Acetylation is an effective method for changing wood–water interactions [10,11]. The acetylation of wood is typically carried out by the use of acetic anhydride. The reaction of wood with the acetic anhydride results in the substitution of hydrophilic hydroxyl groups with less hydrophilic acetyl groups [9,12,13]. In addition, acetylation also bulks wood cell walls [14,15]. Wood after acetylation

shows lower wettability, equilibrium moisture content [15,16], and water uptake [13]. In addition, dimensional stability [17–19] and resistance to decay [12,20,21] are prominently improved. As a result of these advantageous properties, acetylation has been developed to the industrial scale and commercialized [22].

Wood–water interactions are related to the biopolymer composition of wood. Cellulose makes up about 40–50% of the dry weight of wood, and it has a higher hydroxyl concentration than hemicelluloses and lignin [8,23,24]. However, cellulose microfibrils are highly compact, and only the hydroxyl groups on the microfibril surfaces are accessible to water [25,26]; thus, the hydroxyl accessibility is lower than the theoretical value [27]. Hemicelluloses are amorphous and can be found in the matrix between cellulose fibrils [28]. They account for about 20–35% of the dry mass of wood [29,30]. Due to the easier accessibility of hydroxyl groups, hemicelluloses are regarded as one of the most hygroscopic components in plant biomass [27,31,32]. Lignin is a three-dimensional heteropolymer primarily composed of phenyl propane units through carbon–carbon bonds or ether bonds, and some hydroxyl groups can also be found. In wood cell walls, lignin mainly surrounds the cellulose and hemicelluloses [23,29]. Since lignin has lower hydroxyl content than hemicelluloses, its hydroxyl accessibility is also lower [27]. Based on the findings that the number of accessible hydroxyl groups differs among cellulose, hemicelluloses, and lignin [27,31–33], we hypothesize that biopolymer composition also affects the acetylation result.

The objective of this study was to investigate how changes in the biopolymer composition in wood as well as acetylation affect the hydroxyl accessibility, moisture content, and water distribution in the material.

2. Materials and Methods

2.1. Materials

Wood samples were taken from the sapwood of a poplar (*Populus euramericana* Cv.) harvested from the Greater Khingan Mountains in China. All samples were cut into specimens sized 20 mm in both tangential and radial directions and 4 mm along the longitudinal direction, and no defects could be observed on the specimens. The average air-dried density of the specimens was about 0.36 g cm^{-3} , and the average ring width was about 3.5 mm.

2.2. Methods

The specimens were vacuum-dried at $65 \text{ }^{\circ}\text{C}$ for 48 h until constant weight, and the oven-dried mass of each specimen was recorded. Then, the experimental design as shown in Figure 1 was followed. First, specimens were extracted using a mixture of ethanol and benzene (1:2 volume ratio). For half of the extracted specimens, hemicelluloses were then partially removed using the hydrothermal treatment at $180 \text{ }^{\circ}\text{C}$ in a reactor (KH-200, Shanghai Tianheng Instrument Co., Ltd. Shanghai, China) for 2 h with a water-to-solid ratio of 20:1 (*w/w*). For the other half of the specimens, delignification was performed by placing the specimens in a vacuum of -0.1 MPa for half an hour; then, a mixture of 967 mL of distilled water and 20 g of sodium hypochlorite mixed with 13 mL of acetic acid were added, while the vacuum of -0.1 MPa was still running for 4.5 h. Afterwards, the flask with the specimens were subjected to a water bath at $40 \text{ }^{\circ}\text{C}$ for 30 h. Then, all the specimens were rinsed with running water for 24 h and air-dried for 48 h [34]. After treatments, specimens were dried in a vacuum oven at $80 \text{ }^{\circ}\text{C}$ for 48 h. Based on the total dry mass of wood after extraction, the difference in mass of each specimen was used to calculate hemicellulose and lignin loss [34].

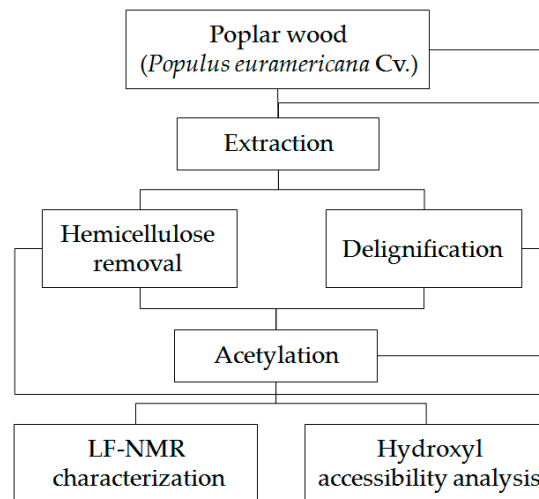


Figure 1. Schematic diagram of the general experimental design.

2.2.1. Acetylation

The specimens were subjected to 15 min vacuum treatment at about -0.1 MPa, and then a mixture of pyridine and acetic anhydride (volume ratio 5:2) was injected into the reaction flask. Additionally, to investigate if pyridine itself affects the measurements, control specimens were produced for which only pyridine was injected. After leaving specimens in the liquid for 1 h at ambient temperature, the reaction flasks were heated using an oil bath at 80 °C for 1 h using a magnetic stirrer to ensure circulation. At the end of the reaction period, the flask was removed from the oil bath, the hot reagent was decanted off, and ice-cold acetone was added to quench the reaction. Afterwards, residual chemicals were removed by washing, first in pure acetone and then in the mixture of acetone and distilled water (1:1 volume ratio), and finally in distilled water. During the whole washing process, a magnetic stirrer was used to accelerate the washing of residual chemicals. Finally, the specimens were air-dried for 48 h at ambient conditions and then vacuum-dried at 65 °C for 48 h, after which the oven-dried mass was measured. The degree of acetylation was calculated based on the relative increase in mass of each specimen prior to and after acetylation. That is, for the delignified specimens and specimens where hemicellulose was partially removed, the mass after delignification/hemicellulose removal was used when calculating the degree of acetylation.

2.2.2. Low-Field Nuclear Magnetic Resonance (LFNMR) Characterization

The dried specimens were vacuum saturated with water by placing the specimens in reaction flasks, applying vacuum (2.8–3.2 kPa) for 30 min, and injecting deionized water into the reaction flask while still running the vacuum pump. Then, the vacuum pump was run for 2 h with the specimens in water before atmospheric pressure was applied. The specimens were kept in water for at least 2 days before the LFNMR measurements were performed.

Before placing the specimens in the LFNMR tube, each specimen was wiped on a wet piece of cloth to avoid the presence of free water on the specimen surface but without drying the specimen, in accordance with previous study [35]. Two specimens were placed on top of each other in the LFNMR tube; then, the LFNMR tube with specimens inside was sealed with a Teflon rod, and the mass of the whole set was determined. Before each measurement, the LFNMR tube with the specimens and Teflon rod was kept in the instrument (mq20-Minispec, Bruker, Billerica, MA, USA) for 10 min to allow temperature equilibration. All measurements were performed at 20 °C. The Carr–Purcell–Meiboom–Gill (CPMG) pulse sequence [36,37] was used to determine the T_2 relaxation time with a pulse separation (τ) of 0.1 ms, 15,000 echoes, gain 84 dB, 8 scans, and a recycle delay of 5 s. After measurement, the LFNMR tube and Teflon rod were weighed to calculate the mass of the water saturated wood specimens. Then, the specimens were dried in a vacuum oven at 80 °C to get the oven-dried mass. The moisture content

of each specimen was determined as the mass of water divided by the dry mass of the specimen. For the acetylated specimens, the moisture content was corrected for the increase in dry mass caused by the acetylation, also taking into account the mass loss of the pyridine control specimens. The amount of replicates used for the LFNMR measurements is shown in Table 1. Note that for the LFNMR measurements, one replicate consists of two specimens inside the LFNMR tube. The CPMG decay curves were analyzed by exponential decay analysis using the non-negative least squares (NNLS) fitting algorithm of the software PROSPA [9]. The moisture content represented by each peak (u_i) was calculated according to Equation (1) as below.

$$u_i = u \cdot \left(\frac{S_i}{S_{\text{tot}}} \right) \quad (1)$$

where u (%) is the total moisture content of the water saturated wood, S_i is the integral of the peak component i , and S_{tot} is the total integral of all the peaks. The integrals were determined as $dS/d(\ln T_2)$ [38].

2.2.3. Hydroxyl Accessibility

A sorption balance (DVS Advantage, Surface Measurement Systems, London, UK) was used to measure the hydroxyl accessibility [27]. The wood specimens were cut into thin slices with a razor blade, and approximately 10 mg of the material was used for each measurement. The sample was placed in the sample pan and initially dried at 60 °C for 6 h using the pre-heater followed by a temperature stabilization period of 1 h at 25 °C and 0% relative humidity (RH). Then, the sample was exposed to deuterium oxide (99.9%-atom, Sigma Aldrich Chemie GmbH, Buchs, Switzerland) vapor at 95% RH/25 °C for 10 h, and it was then dried again at 60 °C for 6 h using the pre-heater. Again, a temperature stabilization period of 1 h was used before the dry mass was taken. The temperature increase between 25 and 60 °C and then back to 25 °C was in both cases obtained by a linear increase/decrease in temperature over a period of 10 min. Thus, the total time of measurement for one sample was 24 h and 40 min. Then, the hydroxyl accessibility, c_{acc} (mmol g⁻¹), was determined based on the dry masses before and after deuteration according to the following equation [11]:

$$c_{\text{acc}} = \frac{(m_{\text{ex}} - m_{\text{or}})}{\Delta M_{\text{HD}} m_{\text{or}}} (1 + R_{\text{mod}}) \cdot 1000 \quad (2)$$

where m_{ex} (g) is the dry mass of the sample after the deuterium exchange process, m_{or} (g) is the original dry mass of the wood sample prior to the exchange process, ΔM_{HD} (g mol⁻¹) is the difference in molar mass between protium (¹H) and deuterium (²H), and R_{mod} (g g⁻¹) is the relative mass gain from acetylation. Multiplication with $(1 + R_{\text{mod}})$ puts the hydroxyl accessibility in relation to the dry mass of the non-modified material, i.e., it removes the influence of the additional mass due to the modification chemical [10,11]. The number of replicates used in different groups is shown in Table 1.

Table 1. Replicates of control wood (C), wood with low hemicelluloses (LH), wood with low lignin (LL), pyridine-treated wood (PC), acetylated wood (AC), acetylated wood with low hemicelluloses (AH), and acetylated wood with low lignin (AL) used for different tests. LFNMR: low-field nuclear magnetic resonance.

Test	Replicate								
	C	PC	AC	LH	PH	AH	LL	PL	AL
LFNMR characterization	3	3	3	3	1	1	3	1	1
Hydroxyl accessibility	3	3	3	4	3	3	3	3	3

Based on the chemical substitution of hydroxyl groups with acetyl groups during acetylation [11], the theoretical hydroxyl accessibility can be calculated from the mass change of wood. The theoretical

hydroxyl accessibility, $c_{\text{acc,theo}}$ of acetylated wood (AC_C), acetylated wood with low hemicelluloses (AH_C), and acetylated wood with low lignin (AL_C) were determined according to the equation as below.

$$c_{\text{acc,theo}} = c_{\text{acc,0}} - \frac{(m_{\text{ac}} - m_0)}{M_{\text{ac}}} \cdot 1000 \quad (3)$$

Here, $c_{\text{acc,0}}$ (mmol g^{-1}) is the hydroxyl accessibility of untreated wood, m_{ac} (g) is the dry mass of the wood after acetylation, m_0 (g) is the original dry mass of the wood prior to acetylation, and M_{ac} (g mol^{-1}) is the added molar mass by acetyl group reacting with a hydroxyl, i.e., the molar mass of COCH_3 subtracted by the molar mass of H, which yields 42.04 g mol^{-1} . Furthermore, the possibility of mass loss during acetylation was investigated by taking the mass gain from acetylation as the sum of the measured mass increase and the absolute value of the mass loss in pyridine control specimens.

3. Results

3.1. General Mass Changes of Wood after Treatments

Table 2 gives the mass change of wood after different treatments. After partial hemicellulose removal and delignification, the hemicellulose loss was about 8.6% of the total dry weight, and the lignin loss was about 8.9% of the total dry weight, respectively. Based on the hemicelluloses and lignin content in *Populus adenopoda* Maxim. in previous literature [39], an estimation could be given that about 38.0% and 34.4% of the original hemicelluloses and lignin were removed, respectively. The acetylation led to a mass gain of about 15% for all three treatments, which in reality was somewhat larger, as pyridine alone gave a mass reduction of about 2–4%; see Table 2.

Table 2. Mass changes of wood after different treatments.

Specimen	Control Wood	Partially Hemicellulose-Depleted	Partially Delignified
Mass change, pretreatment (% g g^{-1}) ^a	0	−8.6 (+/−0.1)	−8.9 (+/−0.1)
Mass change, acetylation (% g g^{-1}) ^a	15.7 (+/−0.4) ^b	15.3 (+/−0.7) ^c	14.9 (+/−0.8) ^d

^a Data provided as the average and standard deviation in parentheses. ^b Mass change from control wood in pure pyridine was -2.5 (+/−0.4) % g g^{-1} . ^c Mass change from partially hemicellulose-depleted wood in pure pyridine was -2.7 (+/−0.4) % g g^{-1} . ^d Mass change from partially delignified wood in pure pyridine was -4.2 (+/−0.4) % g g^{-1} .

3.2. Effect of Hemicellulose Content Reduction on the Moisture in Acetylated Wood

Continuous T_2 (spin-spin) distributions for control wood (C), wood with low hemicelluloses (LH), pyridine-treated wood (PC), acetylated wood (AC), and acetylated wood with low hemicelluloses (AH) are shown in Figure 2. The part of the spectrum with T_2 lower than about 10 ms was attributed to the water within cell walls. Peak 3 between 10 and 100 ms was assigned to the water in small voids or small cavities (defined as void water here), and Peak 4 above 100 ms represented water in cell lumina [35]. Four peaks were visible in the T_2 distribution of the control specimens, while after pyridine treatment, the wood exhibited three peaks and only one peak representing cell wall water. After partial hemicellulose removal, the T_2 peaks for the cell wall water shifted toward longer times, while the T_2 of Peaks 3 and 4 became shorter. After acetylation, the T_2 of all peaks shifted toward longer times. The relative intensity of T_2 peaks of AH was decreased by hemicellulose removal and acetylation, and the T_2 of cell wall water, void water, and cell lumen water became longer. Additionally, AH generally exhibited longer T_2 than AC.

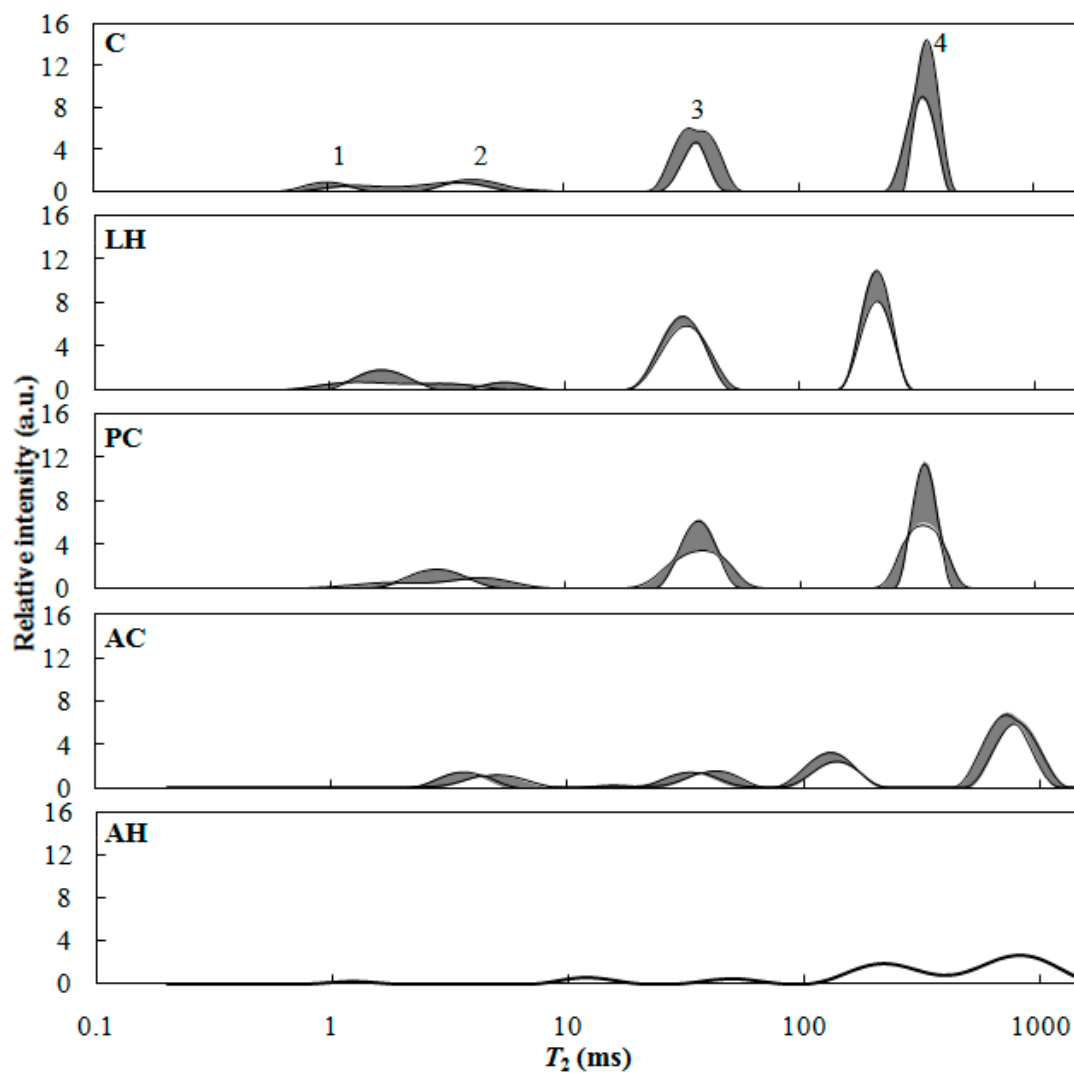


Figure 2. Continuous T_2 (spin–spin) distributions for control wood (C), wood with low hemicelluloses (LH), pyridine-treated wood (PC), acetylated wood (AC), and acetylated wood with low hemicelluloses (AH). Gray filled areas represent mean values including standard deviation.

Based on the peak integral area of the total area analyzed by LFNMR, the cell wall moisture content of the differently treated wood can be calculated and compared, but the absolute value of the cell wall moisture content is most probably under-estimated [9]. As shown in Figure 3, partial hemicellulose removal slightly reduced the cell wall moisture content, but not to a large extent. A similar, slightly reduced moisture content was seen for the pyridine treated specimens. However, acetylation led to a substantial reduction, and compared with control wood, the cell wall moisture content of AC was lowered by about 24%. In addition, partial hemicellulose removal in combination with acetylation seemed to further lower the cell wall moisture content. However, these results should be interpreted with care, since only one replicate was used for AH.

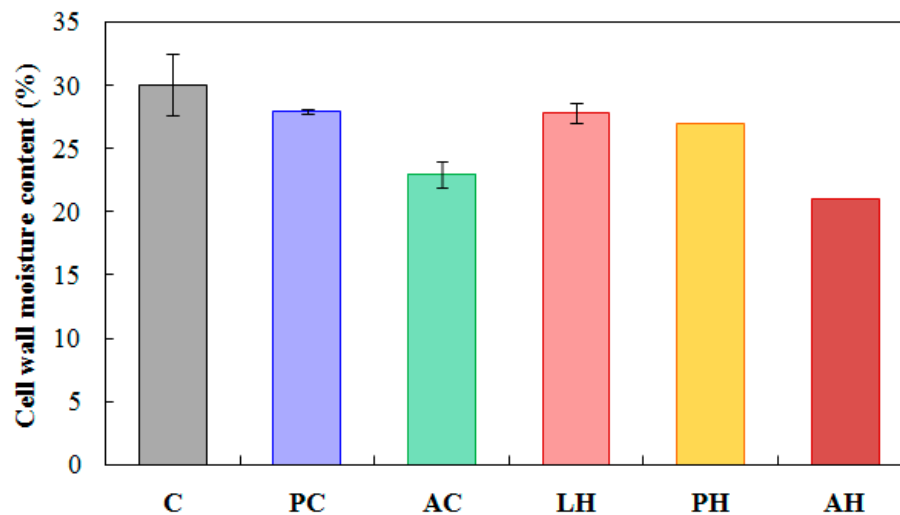


Figure 3. Cell wall moisture content in water-saturated control wood (C), pyridine-treated wood (PC), acetylated wood (AC), wood with low hemicelluloses (LH), pyridine-treated wood with low hemicelluloses (PH), and acetylated wood with low hemicelluloses (AH) analyzed by LFNMR.

The hydroxyl accessibility data are shown in Figure 4. Hemicellulose removal gave a decrease in hydroxyl accessibility, while the pyridine treatment alone had almost no effect as expected. After acetylation, the hydroxyl accessibility of AC decreased by about 45%. Based on the chemical substitution reaction between acetic anhydride and wood, the hydroxyl accessibility was calculated, and the result is included in Figure 4 for comparison. The theoretical hydroxyl accessibility of acetylated wood (ACc) shows about 58% reduction compared with the control wood, which was slightly larger than the experimental results. The partial hemicellulose removal decreased the measured hydroxyl accessibility of acetylated wood, and AH exhibited much lower hydroxyl accessibility than control wood (by about 91%), while the theoretical estimate was only about 69% reduced.

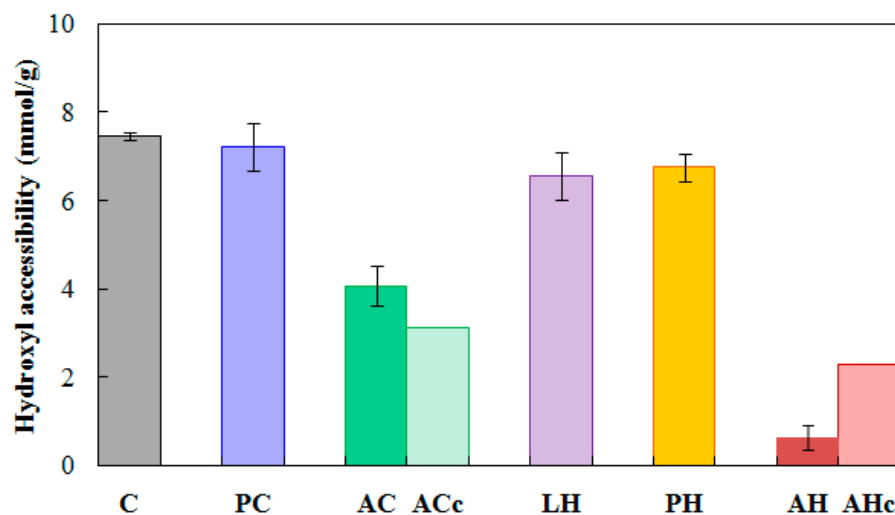


Figure 4. Hydroxyl accessibility of differently treated wood. ACc: the calculated hydroxyl accessibility of AC. AHc: the calculated hydroxyl accessibility of AH.

3.3. Effect of Lignin Content Reduction on the Moisture in Acetylated Wood

To investigate the effect of lignin content reduction on moisture in acetylated wood, the continuous T_2 (spin–spin) distributions for control wood (C), wood with low lignin (LL), pyridine-treated wood (PC), acetylated wood (AC), and acetylated wood with low lignin (AL) are illustrated in Figure 5. Partial delignification had no effect on the number of T_2 peaks, i.e., four peaks were observed also in

the continuous T_2 (spin–spin) distributions for LL. However, the T_2 of all peaks was shorter. Compared to control wood and partially delignified wood, the AL exhibited longer T_2 assigned to all peaks. In addition, the T_2 of cell wall water of AL was even slightly longer than that of AC, while the T_2 of cell lumen water was shorter.

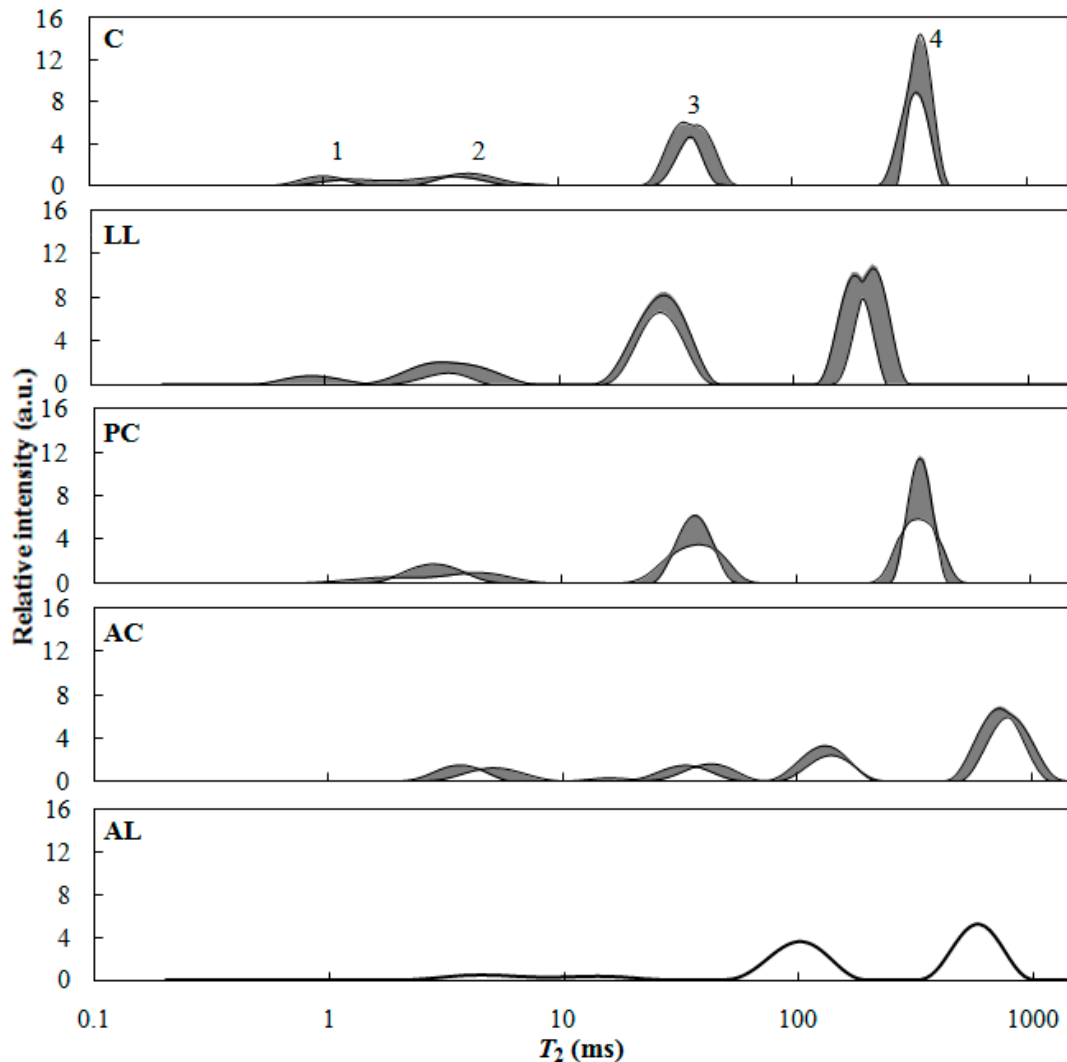


Figure 5. Continuous T_2 (spin–spin) distributions for control wood (C), wood with low lignin (LL), pyridine-treated wood (PC), acetylated wood (AC), and acetylated wood with low lignin (AL). Gray filled areas represent mean values including standard deviation.

The corresponding cell wall moisture content of saturated wood after different treatments is presented in Figure 6. In contrast to LH, LL showed higher cell wall moisture content than control wood and pyridine treated wood. After further acetylation, the cell wall moisture content of pre-delignified wood decreased and was close to that of the control wood. Nonetheless, the AL still had higher cell wall moisture content than AC, which was similar to the trend between control wood and partially delignified wood.

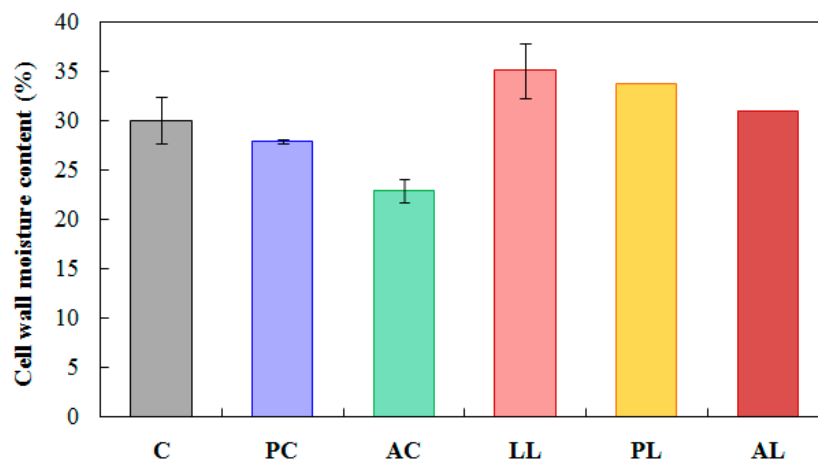


Figure 6. Cell wall moisture content in saturated control wood (C), pyridine-treated wood (PC), acetylated wood (AC), wood with low lignin (LL), pyridine-treated wood with low lignin (PL), and acetylated wood with low lignin (AL) analyzed by LFNMR.

Figure 7 presents the hydroxyl accessibility of wood after different treatments determined gravimetrically as well as theoretical estimates for acetylated wood and for acetylated wood with low lignin. The LL had higher hydroxyl accessibility than the control wood and pyridine-treated wood. Acetylation of the pre-delignified wood gave a marked reduction, and the experimentally determined hydroxyl accessibility of the AL was lower than the control wood by about 88%, while the calculated theoretical hydroxyl accessibility was much larger similar to the results seen for hemicellulose-depleted wood.

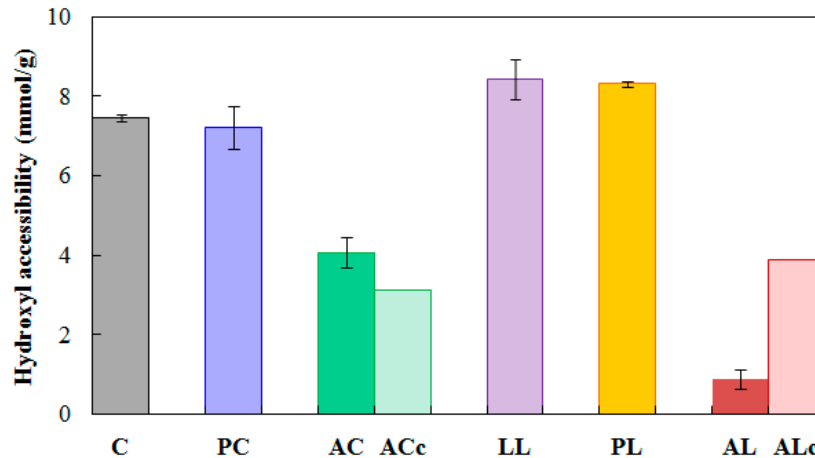


Figure 7. Hydroxyl accessibility of control wood (C), pyridine-treated wood (PC), acetylated wood (AC), wood with low lignin (LL), pyridine-treated wood with low lignin (PL), and acetylated wood with low lignin (AL). ACc: the calculated hydroxyl accessibility of AC. ALc: the calculated hydroxyl accessibility of AL.

4. Discussion

Similar to some hardwoods in previous studies [40], poplar wood had more than one cell wall water population (Figure 2). This can possibly be attributed to varying environments where cell wall water occurs, for instance either cell walls of different types of angiosperm xylem cells or different environments within the same cell wall.

Hemicellulose removal gave a slight reduction in hydroxyl accessibility (Figure 4) of the remaining wood, which was expected as accessible hydroxyl groups are abundant in this biopolymer [31,32]. Partial hemicellulose removal can enlarge the size of some pores in cell walls [41,42]. This is possibly

the reason for the longer T_2 for cell wall water obtained in the present study after partial hemicellulose removal in accordance with previous research [43]. The shorter T_2 for void water and cell lumen water of LH may be caused by physical changes such as the deformation or collapse of some voids and cell lumens during treatments [43]. However, there was only a slight but no clear reduction in cell wall moisture content (Figure 3). For the pyridine controls, there were no clear effects on the hydroxyl accessibility (Figure 4) and the cell wall moisture content (Figure 3), although the cell wall moisture content is possibly slightly lower for the pyridine-treated controls. However, pyridine is an excellent swelling agent [9], so the observed disappearance of one cell wall water peak in the LFNMR results might be due to the porosity changes after the swelling of the cell walls. The longer T_2 for cell wall water, void water, and cell lumen water in acetylated wood is consistent with previous research [9,44]. These changes are most probably related to a change in chemical environment rather than physical environment, since acetylation does not change the size of the macro voids in the wood structure. However, it is possible that acetylation can introduce micro cracks in the cell wall [45]. By contrast, a weaker wood affinity to water in AH than AC is suggested by the T_2 of the peak position. The reason for this seems to be a synergistic effect of hemicellulose removal and acetylation, especially for the decrease of the hydroxyl accessibility (Figure 4). In addition, the cell wall moisture content of AH was lower than that of AC, and a decrease of over 30% can be found when comparing AH with control wood.

Lignin and hemicellulose removal had different effects on the moisture in wood. Partial delignification increased the wood affinity to water implied by the shorter T_2 for cell wall water, void water, and cell lumen water (Figure 5). This can be at least partly explained by the higher hydroxyl accessibility of LL than of control wood (Figure 7). A higher cell wall moisture content can be seen in LL than in control wood, which is in accordance with previous research on the effects of lignin on wood moisture content [46,47]. Similar to the effects of acetylation on control wood, the LL after acetylation also gave longer T_2 for cell wall water, void water, and cell lumen water. AL also exhibited lower cell wall moisture content than LL. In addition, partial lignin removal contributed to the increase of T_2 for cell wall water of acetylated wood, corresponding to the larger pore size of acetylated wood caused by delignification. Some researchers have utilized such increase in porosity in the creation of wood materials with novel functionalities [48–51]. The shorter T_2 for cell lumen water of AL implies that partial lignin removal can increase the affinity to water of acetylated wood.

As expected, the observed moisture distributions and moisture contents in different water pools within wood were affected by both the physical and the chemical environment within the wood cell walls, and hemicellulose removal or delignification changed both of these. Similar to some previous cases [15,43], the physical change (i.e., porosity) and chemical change (i.e., molecular groups) occur simultaneously, and interpretation of the results has to incorporate both.

The results for hydroxyl accessibility showed that for the acetylated control wood, the theoretical estimate and the values obtained from measurements are rather similar, although the theoretical value is lower. However, for the two acetylated biopolymer-depleted samples, the estimated value is substantially higher. This suggests a synergistic effect not included in the theoretical estimate. Since the same trend is seen both when the most hydrophilic (hemicelluloses) and when the least hydrophilic (lignin) biopolymer is partially removed, we speculate that it is the increased porosity of the cell wall prior to acetylation that makes the acetylation more efficient, i.e., better at covering access to hydroxyl groups not only by the direct binding of acetyl groups to hydroxyl groups, but also by sterically hindering access to hydroxyl groups further inside the pores. From the deuteration experiments, this is seen to be the case for water in the vapor form at a partial pressure corresponding to 95% RH. However, when comparing to the LFNMR results for cell wall water contents obtained after saturation with liquid water by use of vacuum impregnation, the combined effect of biopolymer removal and acetylation is much smaller. These data strengthen prior results, highlighting the need to distinguish between wood cell wall saturation by vapor or liquid water, as these two situations are very different [27,52].

5. Conclusions

Hemicelluloses or lignin were partially removed from poplar wood to investigate the effects of changes in biopolymer composition on moisture in wood before and after acetylation. As expected, acetylation of pyridine-swelled wood made the wood cell wall less accessible to water and led to over 24% reduction of cell wall moisture content in the water-saturated wood. Partial hemicellulose removal reduced the cell wall moisture content in water-saturated wood, while partial delignification increased it. The cell wall moisture content changes of wood after treatments were mirrored by the hydroxyl accessibility variation. When the modified wood types were acetylated, the amount of cell wall water in water-saturated wood was further reduced for both. The hydroxyl accessibility was at the same time substantially reduced.

Author Contributions: Conceptualization, T.Y., E.E.T., M.F. and L.G.T.; Data curation, T.Y.; Funding acquisition, E.E.T., M.F. and J.C.; Investigation, T.Y., E.E.T., M.F., J.C., R.D. and L.G.T.; Methodology, E.E.T., M.F., J.C. and L.G.T.; Software, E.E.T.; Supervision, E.E.T., M.F., E.M., J.C. and L.G.T.; Validation, T.Y.; Writing—original draft, T.Y.; Writing—review & editing, E.E.T., M.F., E.M., J.C., R.D. and L.G.T. All authors have read and agreed to the published version of the manuscript.

Funding: This research was funded by the European Regional Development Fund Interreg Öresund-Kattegat-Skagerrak grant number 20201851, SNS Nordic Forest Research grant number SNS-125, National Key Research and Development Program of China grant number 2017YFD0600203, and Fundamental Research Funds for the Central Universities of China grant number 2019JQ03013.

Conflicts of Interest: The authors declare no conflict of interest.

References

- Sathre, R.; Gustavsson, L. Using wood products to mitigate climate change: External costs and structural change. *Appl. Energy* **2009**, *86*, 251–257. [[CrossRef](#)]
- Wang, L.; Toppinen, A.; Juslin, H. Use of wood in green building: A study of expert perspectives from the UK. *J. Clean. Prod.* **2014**, *65*, 350–361. [[CrossRef](#)]
- Milner, H.; Woodard, A. Sustainability of engineered wood products. In *Sustainability of Construction Materials*, 2nd ed.; Khatib, J.M., Ed.; Woodhead Publishing: Sawston Cambridge, UK, 2016; pp. 159–180.
- Skaar, C. *Wood-Water Relations*; Springer: Berlin, German, 1988.
- Kong, L.; Guan, H.; Wang, X. In Situ Polymerization of Furfuryl Alcohol with Ammonium Dihydrogen Phosphate in Poplar Wood for Improved Dimensional Stability and Flame Retardancy. *ACS Sustain. Chem. Eng.* **2018**, *6*, 3349–3357. [[CrossRef](#)]
- Wagner, L.; Bos, C.; Bader, T.K.; De Borst, K. Effect of Water on the Mechanical Properties of Wood Cell Walls—Results of a Nanoindentation Study. *Bioresources* **2015**, *10*, 4011–4025. [[CrossRef](#)]
- Thybring, E.E.; Kymäläinen, M.; Rautkari, L. Moisture in modified wood and its relevance for fungal decay. *iForest Biogeosci. For.* **2018**, *11*, 418–422. [[CrossRef](#)]
- Rowell, R.M. Chemical modification of wood. In *Wood Chemistry and Wood Composites*; Taylor & Francis: Boca Raton, FL, USA, 2005.
- Beck, G.; Thybring, E.E.; Thygesen, L.G.; Hill, C. Characterization of moisture in acetylated and propionylated radiata pine using low-field nuclear magnetic resonance (LFNMR) relaxometry. *Holzforschung* **2018**, *72*, 225–233. [[CrossRef](#)]
- Hill, C.A.S. The reduction in the fibre saturation point of wood due to chemical modification using anhydride reagents: A reappraisal. *Holzforschung* **2008**, *62*, 423–428. [[CrossRef](#)]
- Popescu, C.-M.; Hill, C.A.S.; Curling, S.; Ormondroyd, G.; Xie, Y. The water vapour sorption behaviour of acetylated birch wood: How acetylation affects the sorption isotherm and accessible hydroxyl content. *J. Mater. Sci.* **2013**, *49*, 2362–2371. [[CrossRef](#)]
- Hill, C.A.S. *Wood Modification: Chemical, Thermal and Other Processes*; John Wiley & Sons: West Sussex, UK, 2006.
- Moghaddam, M.S.; Wälinder, M.E.; Claesson, P.M.; Swerin, A. Wettability and swelling of acetylated and furfurylated wood analyzed by multicycle Wilhelmy plate method. *Holzforschung* **2016**, *70*, 69–77. [[CrossRef](#)]

14. Papadopoulos, A.N.; Hill, C.A.S. The biological effectiveness of wood modified with linear chain carboxylic acid anhydrides against *Coniophora puteana*. *Holz Roh Werkst.* **2002**, *60*, 329–332. [[CrossRef](#)]
15. Beck, G.; Strohbusch, S.; Larnøy, E.; Militz, H.; Hill, C. Accessibility of hydroxyl groups in anhydride modified wood as measured by deuterium exchange and saponification. *Holzforschung* **2017**, *72*, 17–23. [[CrossRef](#)]
16. Rowell, R.M.; Simonson, R.; Hess, S.; Plackett, D.V.; Cronshaw, D.; Dunningham, E. Acetyl distribution in acetylated whole wood and reactivity of isolated wood cell-wall components to acetic anhydride. *Wood Fiber Sci.* **1994**, *26*, 11–18.
17. Ramsden, M.J.; Blake, F.S.R.; Fey, N.J. The effect of acetylation on the mechanical properties, hydrophobicity and dimensional stability of *Pinus sylvestris*. *Wood Sci. Technol.* **1997**, *31*, 97–104. [[CrossRef](#)]
18. Chang, H.-T.; Chang, S.-T. Moisture excluding efficiency and dimensional stability of wood improved by acylation. *Bioresour. Technol.* **2002**, *85*, 201–204. [[CrossRef](#)]
19. Rowell, R.M. Dimensional stability and fungal durability of acetylated wood. *Komunikaty* **2016**, *59*, 139–150.
20. Stamm, A.J.; Baechler, R.H. Decay resistance and dimensional stability of five modified woods. *For. Prod. J.* **1960**, *10*, 22–26.
21. Zelinka, S.L.; Kirker, G.T.; Bishell, A.B.; Glass, S.V. Effects of Wood Moisture Content and the Level of Acetylation on Brown Rot Decay. *Forests* **2020**, *11*, 299. [[CrossRef](#)]
22. Mantanis, G. Chemical Modification of Wood by Acetylation or Furfurylation: A Review of the Present Scaled-up Technologies. *Bioresources* **2017**, *12*, 4478–4489. [[CrossRef](#)]
23. Forest Products Laboratory. *Wood Handbook—Wood as an Engineering Material*; Forest Products Laboratory: Madison, WI, USA, 1999; p. 463.
24. Hoadley, R.B. *Understanding Wood: A Craftsman's Guide to Wood Technology*; The Taunton Press: Newtown, CT, USA, 2000.
25. Maréchal, Y.; Chanzy, H. The hydrogen bond network in Iβ cellulose as observed by infrared spectrometry. *J. Mol. Struct.* **2000**, *523*, 183–196. [[CrossRef](#)]
26. Hofstetter, K.; Hinterstoisser, B.; Salmén, L. Moisture uptake in native cellulose—The roles of different hydrogen bonds: A dynamic FT-IR study using Deuterium exchange. *Cellulose* **2006**, *13*, 131–145. [[CrossRef](#)]
27. Thybring, E.E.; Thygesen, L.G.; Burgert, I. Hydroxyl accessibility in wood cell walls as affected by drying and re-wetting procedures. *Cellulose* **2017**, *60*, 665–2384. [[CrossRef](#)]
28. Kulasinski, K.; Guyer, R.; Ketten, S.; Derome, D.; Carmeliet, J. Impact of Moisture Adsorption on Structure and Physical Properties of Amorphous Biopolymers. *Macromolecules* **2015**, *48*, 2793–2800. [[CrossRef](#)]
29. Ek, M.; Gellerstedt, G.; Henriksson, G. *Wood Chemistry and Wood Biotechnology*; De Gruyter: Berlin, Germany, 2009.
30. Asif, M. Sustainability of timber, wood and bamboo in construction. In *Sustainability of Construction Materials*; Woodhead Publishing Limited: Cambridge, UK, 2009.
31. Christensen, G.N.; Kelsey, K.E. The rate of sorption of water vapor by wood. *Holz Roh Werkst* **1959**, *17*, 178–188. [[CrossRef](#)]
32. Engelund, E.T.; Thygesen, L.G.; Svensson, S.; Hill, C.A.S.; Thybring, E.E. A critical discussion of the physics of wood–water interactions. *Wood Sci. Technol.* **2012**, *47*, 141–161. [[CrossRef](#)]
33. Ringman, R.; Beck, G.; Pilgård, A. The Importance of Moisture for Brown Rot Degradation of Modified Wood: A Critical Discussion. *Forests* **2019**, *10*, 522. [[CrossRef](#)]
34. Yang, T.; Zhou, H.; Ma, E.; Wang, J. Effects of removal of different chemical components on moisture sorption property of *Populus euramericana* Cv. under dynamic hygrothermal conditions. *Results Phys.* **2018**, *10*, 61–68. [[CrossRef](#)]
35. Fredriksson, M.; Thygesen, L.G. The states of water in Norway spruce (*Picea abies* (L.) Karst.) studied by low-field nuclear magnetic resonance (LFNMR) relaxometry: Assignment of free-water populations based on quantitative wood anatomy. *Holzforschung* **2017**, *71*, 77–90. [[CrossRef](#)]
36. Carr, H.Y.; Purcell, E.M. Effects of Diffusion on Free Precession in Nuclear Magnetic Resonance Experiments. *Phys. Rev.* **1954**, *94*, 630–638. [[CrossRef](#)]
37. Meiboom, S.; Gill, D. Modified Spin-Echo Method for Measuring Nuclear Relaxation Times. *Rev. Sci. Instrum.* **1958**, *29*, 688. [[CrossRef](#)]
38. Terenzi, C.; Prakobna, K.; Berglund, L.A.; Furo, I. Nanostructural Effects on Polymer and Water Dynamics in Cellulose Biocomposites: ²H and ¹³C NMR Relaxometry. *Biomacromolecules* **2015**, *16*, 1506–1515. [[CrossRef](#)]

39. Liu, H.E.; Liu, L.; Si, H.G.; Feng, H.; Han, Y.F. Chemical composition of wood of some Poplars. *J. Zhejiang For. Coll.* **1995**, *12*, 342–346.
40. Elder, T.; Labbé, N.; Harper, D.P.; Rials, T. Time domain-nuclear magnetic resonance study of chars from southern hardwoods. *Biomass Bioenergy* **2006**, *30*, 855–862. [[CrossRef](#)]
41. Yin, J.; Yuan, T.; Lu, Y.; Song, K.; Li, H.; Zhao, G.; Yin, Y. Effect of compression combined with steam treatment on the porosity, chemical composition and cellulose crystalline structure of wood cell walls. *Carbohydr. Polym.* **2017**, *155*, 163–172. [[CrossRef](#)] [[PubMed](#)]
42. Yang, T.; Wang, J.; Xu, J.; Ma, E.; Cao, J. Hygroscopicity and dimensional stability of *Populus euramericana* Cv. modified by furfurylation combined with low hemicellulose pretreatment. *J. Mater. Sci.* **2019**, *54*, 13445–13456. [[CrossRef](#)]
43. Elder, T.; Houtman, C. Time-domain NMR study of the drying of hemicellulose extracted aspen (*Populus tremuloides* Michx.). *Holzforschung* **2013**, *67*, 405–411. [[CrossRef](#)]
44. Thygesen, L.G.; Elder, T. Moisture in untreated, acetylated, and furfurylated Norway spruce studied during drying using time domain NMR. *Wood Fiber Sci.* **2013**, *40*, 309–320.
45. Wålinder, M.; Omidvar, A.; Seltman, J.; Segerholm, K. Micromorphological studies of modified wood using a surface preparation technique based on ultraviolet laser ablation. *Wood Mater. Sci. Eng.* **2009**, *4*, 46–51. [[CrossRef](#)]
46. Ou, R.; Xie, Y.; Wolcott, M.P.; Sui, S.; Wang, Q. Morphology, mechanical properties, and dimensional stability of wood particle/high density polyethylene composites: Effect of removal of wood cell wall composition. *Mater. Des.* **2014**, *58*, 339–345. [[CrossRef](#)]
47. Zhou, H.; Li, J.; Ma, E. Static and dynamic sorption of lignin removed *Populus euramericana*. *Tappi J.* **2018**, *17*, 71–77. [[CrossRef](#)]
48. Li, Y.; Fu, Q.; Yu, S.; Yan, M.; Berglund, L. Optically Transparent Wood from a Nanoporous Cellulosic Template: Combining Functional and Structural Performance. *Biomacromolecules* **2016**, *17*, 1358–1364. [[CrossRef](#)]
49. Zhu, M.; Song, J.; Li, T.; Gong, A.; Wang, Y.; Dai, J.; Yao, Y.; Luo, W.; Henderson, D.; Hu, L. Highly Anisotropic, Highly Transparent Wood Composites. *Adv. Mater.* **2016**, *28*, 5181–5187. [[CrossRef](#)] [[PubMed](#)]
50. Fu, Q.; Medina, L.; Li, Y.; Carosio, F.; Hajian, A.; Berglund, L.A. Nanostructured Wood Hybrids for Fire-Retardancy Prepared by Clay Impregnation into the Cell Wall. *ACS Appl. Mater. Interfaces* **2017**, *9*, 36154–36163. [[CrossRef](#)]
51. Wu, J.; Wu, Y.; Yang, F.; Tang, C.; Huang, Q.; Zhang, J. Impact of delignification on morphological, optical and mechanical properties of transparent wood. *Compos. Part A Appl. Sci. Manuf.* **2019**, *117*, 324–331. [[CrossRef](#)]
52. Hoffmeyer, P.; Engelund, E.T.; Thygesen, L.G.; Thybring, E.E. Equilibrium moisture content (EMC) in Norway spruce during the first and second desorptions. *Holzforschung* **2011**, *65*, 875–882. [[CrossRef](#)]



© 2020 by the authors. Licensee MDPI, Basel, Switzerland. This article is an open access article distributed under the terms and conditions of the Creative Commons Attribution (CC BY) license (<http://creativecommons.org/licenses/by/4.0/>).